Carbon nanotube mode-locked optically-pumped semiconductor disk laser

K. Seger,[1,*] N. Meiser, [1] S. Y. Choi,[2] B. H. Jung,[2] D.-I. Yeom,[2] F. Rotermund,[2] O. Okhotnikov, [3] F. Laurell,[1] and V. Pasiskevicius[1]

[1]*KTH Laser Physics, Royal Institute of Technology, Roslagstullsbacken 21, 106 91 Stockholm, Sweden*
[2]*Department of Physics & Division of Energy Systems Research, Ajou University, 443-749 Suwon, South Korea*
[3]*Optoelectronics Research Centre, Tampere University of Technology, P.O. Box 692, FIN-33101 Tampere, Finland*
[*]*ks@laserphysics.kth.se*

Abstract: An optically pumped semiconductor disk laser was mode-locked for the first time by employing a single-walled carbon nanotube saturable absorber. Stable passive fundamental mode-locking was obtained at a repetition rate of 613 MHz with a pulse length of 1.23 ps. The mode-locked semiconductor disk laser in a compact geometry delivered a maximum average output power of 136 mW at 1074 nm.

OCIS codes: (140.7260) Vertical cavity surface emitting lasers; (140.4050) Mode-locked lasers; (160.4236) Nanomaterials.

References and links

1. L. F. Mollenauer, P. V. Mamyshev, J. Gripp, M. J. Neubelt, N. Mamysheva, L. Grüner-Nielsen, and T. Veng, "Demonstration of massive wavelength-division multiplexing over transoceanic distances by use of dispersion-managed solitons," Opt. Lett. **25**(10), 704–706 (2000).
2. D. A. B. Miller, "Rationale and challenges for optical interconnects to electronic chips," Proc. IEEE **88**(6), 728–749 (2000).
3. E. Cassan, D. Marris, M. Rouviere, L. Vivien, and S. Laval, "Comparison between electrical and optical global clock distributions for CMOS integrated circuits," Opt. Eng. **44**, 105402 (2005).
4. A. Bhatnagar, C. Debaes, R. Chen, N. C. Helman, G. A. Keeler, D. Agarwal, H. Thienpont, and D. A. B. Miller, "Receiver-less clocking of a CMOS digital circuit using short optical pulses," in 2002 IEEE/LEOS Annual Meeting; Conference Proceedings, 15th Annual Meeting of the IEEE Lasers & Electro-Optics Society, Glasgow, Scotland, 2002, 127–8.
5. A. V. Mule, E. N. Glytsis, T. K. Gaylord, and J. D. Meindl, "Electrical and optical clock distribution networks for gigascale microprocessors," IEEE Trans. Very Large Scale Integration (VLSI) Systems **10**, 582–594 (2002).
6. T. Udem, R. Holzwarth, and T. W. Hänsch, "Optical frequency metrology," Nature **416**(6877), 233–237 (2002).
7. K. Ohki, S. Chung, Y. H. Ch'ng, P. Kara, and R. C. Reid, "Functional imaging with cellular resolution reveals precise micro-architecture in visual cortex," Nature **433**(7026), 597–603 (2005).
8. M. Kuznetsov, F. Hakimi, R. Sprague, and A. Mooradian, "High-power (>0.5-W CW) diode-pumped vertical-external-cavity surface-emitting semiconductor lasers with circular TEM00 beams," IEEE Photon. Technol. Lett. **9**(8), 1063–1065 (1997).
9. C. Tropper, H. D. Foreman, A. Garnache, K. G. Wilcox, and S. H. Hoogland, "Vertical-external-cavity semiconductor lasers," J. Phys. D **37**(9), R75–R85 (2004).
10. J. Chilla, S. Butterworth, A. Zeitschel, J. Charles, A. Caprara, M. Reed, and L. Spinelli, "High power optically pumped semiconductor lasers," Proc. SPIE **5332**, 143–150 (2004).
11. U. Keller, D. A. B. Miller, G. D. Boyd, T. H. Chiu, J. F. Ferguson, and M. T. Asom, "Solid-state low-loss intracavity saturable absorber for Nd:YLF lasers: an antiresonant semiconductor Fabry-Perot saturable absorber," Opt. Lett. **17**(7), 505–507 (1992).
12. U. Keller, K. J. Weingarten, F. X. Kärtner, D. Kopf, B. Braun, I. D. Jung, R. Fluck, C. Hönninger, N. Matuschek, and J. Aus der Au, "Semiconductor saturable absorber mirrors (SESAMs) for femtosecond to nanosecond pulse generation in solid-state lasers," IEEE J. Sel. Top. Quantum Electron. **2**(3), 435–453 (1996).
13. U. Keller, "Recent developments in compact ultrafast lasers," Nature **424**(6950), 831–838 (2003).
14. U. Keller and A. Tropper, "Passively modelocked surface-emitting semiconductor lasers," Phys. Rep. **429**(2), 67–120 (2006).
15. M. Scheller, T. L. Wang, B. Kunert, W. Stolz, S. W. Koch, and J. V. Moloney, "Passively modelocked VECSEL emitting 682 fs pulses with 5.1 W of average output power," Electron. Lett. **48**(10), 588–589 (2012).
16. A. H. Quarterman, K. G. Wilcox, V. Apostolopoulos, Z. Mihoubi, S. P. Elsmere, I. Farrer, D. A. Ritchie, and A. Tropper, "A passively mode-locked external-cavity semiconductor laser emitting 60-fs pulses," Nat. Photonics **3**(12), 729–731 (2009).

#190130 - $15.00 USD Received 7 May 2013; revised 10 Jul 2013; accepted 10 Jul 2013; published 18 Jul 2013

17. U. Griebner, P. Klopp, M. Zorn, and M. Weyers, "Harmonically and fundamentally mode-locked InGaAs-AlGaAs disk laser generating pulse repetition rates in the 100 GHz or pulse duratrions in the 100-fs range," Proc. SPIE Vol. 8242, 824205 (2012).
18. S. Y. Set, H. Yaguchi, Y. Tanaka, and M. Jablonski, "Laser mode locking using a saturable absorber incorporating carbon nanotubes," J. Lightwave Technol. **22**(1), 51–56 (2004).
19. H.-R. Chen, Y.-G. Wang, C.-Y. Tsai, K.-H. Lin, T.-Y. Chang, J. Tang, and W.-F. Hsieh, "High-power, passively mode-locked Nd:$GdVO_4$ laser using single-walled carbon nanotubes as saturable absorber," Opt. Lett. **36**(7), 1284–1286 (2011).
20. I. H. Baek, S. Y. Choi, H. W. Lee, W. B. Cho, V. Petrov, A. Agnesi, V. Pasiskevicius, D. I. Yeom, K. Kim, and F. Rotermund, "Single-walled carbon nanotube saturable absorber assisted high-power mode-locking of a Ti:sapphire laser," Opt. Express **19**(8), 7833–7838 (2011).
21. F. Rotermund, W. B. Cho, S. Y. Choi, I. H. Baek, J. H. Yim, S. Lee, A. Schmidt, G. Steinmeyer, U. Griebner, D.-I. Yeom, K. Kim, and V. Petrov, "Mode-locking of solid-state lasers by single-walled carbon-nanotube based saturable absorbers," Quantum Electron. **42**(8), 663–670 (2012).
22. J. H. Yim, W. B. Cho, S. Lee, Y. H. Ahn, K. Kim, H. Lim, G. Steinmeyer, V. Petrov, U. Griebner, and F. Rotermund, "Fabrication and characterization of ultrafast carbon nanotube saturable absorbers for solid-state laser mode-locking near 1 μm," Appl. Phys. Lett. **93**(16), 161106 (2008).
23. G. J. Spühler, S. Reffert, M. Haiml, M. Moser, and U. Keller, "Output-coupling semiconductor saturable absorber mirror," Appl. Phys. Lett. **78**(18), 2733–2735 (2001).
24. J. J. LePore, "An improved technique for selective etching of GaAs and $Ga_{1-x}Al_xAs$," J. Appl. Phys. **51**(12), 6441–6442 (1980).
25. O. J. Korovyanko, C.-X. Sheng, Z. V. Vardeny, A. B. Dalton, and R. H. Baughman, "Ultrafast spectroscopy of excitons in single-walled carbon nanotubes," Phys. Rev. Lett. **92**(1), 017403 (2004).
26. R. Grange, M. Haiml, R. Paschotta, G. J. Spühler, L. Krainer, M. Golling, O. Ostinelli, and U. Keller, "New regime of inverse saturable absorption for self-stabilizing passively mode-locked lasers," Appl. Phys. B **80**, 151–158 (2005).

1. Introduction

Ultrafast laser sources with high repetition rates in the range of hundreds of megahertz offer a wide range of applications in communications [1,2], clock generation [3–5], metrology [6] and life sciences [7].

Optically-pumped semiconductor disk lasers (OPSDLs) [8] provide a very promising solution to cover a wide spectral range in the visible and near-infrared (NIR) [9] as they can capitalize on the well-established techniques for bandgap and quantum structure engineering as well as reliable high precision growth methods in semiconductors. High homogeneity of the grown semiconductor gain structures enables straightforward scaling of the average output power in OPSDLs by increasing active aperture size [10], if thermal management is taken care of. The small length of the gain structure and quasi-one-dimensional heat flow in the disk geometry facilitate low thermal lensing and fundamental transversal mode operation even at high pump fluences. This is of crucial importance for stable mode-locked laser operation. On the other hand, the short length of the amplification structure typically consisting of only a few quantum wells contributes to the roundtrip gain of only about 0.1 dB which makes OPSDL rather sensitive to intracavity losses such as those due to mode-locking elements. Semiconductor quantum-well (QW) [11,12] and quantum-dot (QD) saturable absorber mirrors (SESAMs) have been successfully used for mode-locking of OPSDLs [13,14]. Where QDs feature a very low saturation fluence for high-repetition rate mode-locking and an absorption which depends on the QD size and not necessarily the material. High-quality semiconductor quantum-well absorber structures with low non-saturable loss enabled demonstration of passively mode-locked OPSDLs with average powers of up to 5.1 W with a pulse length of 683 fs using a QW-SESAM [15] and pulses as short as 60 fs [16] in fundamental mode-locking schemes as well as pulse repetition rate of 92 GHz with pulses shorter than 200 fs in a harmonic mode-locking scheme [17].

In view of broad potential spectral range of OPSDLs it would be of interest to utilize more universal saturable absorber technology which could operate over the whole near-infrared spectral range employing the same basic absorber material. As recently reported, semiconducting single-walled carbon nanotube saturable absorbers (SWCNT-SAs) offer a potential alternative for high-gain solid-state laser mode-locking over a wide NIR spectral

#190130 - $15.00 USD Received 7 May 2013; revised 10 Jul 2013; accepted 10 Jul 2013; published 18 Jul 2013

range [18]. They do not yet have the optimized ratio of saturable loss to non-saturable loss that SESAM possess, but output powers of 3.6 W with a pulse duration of 8.4 ps at a repetition rate of 122 MHz in a Nd:$GdVO_4$ laser [19] and SWCNT-SA assisted mode-locking with pulses as short as 62 fs in a Ti:Al_2O_3 laser with an output power of 600 mW at a repetition rate of 99.4 MHz [20] have been achieved in fundamentally mode-locked solid-state lasers recently. A more comprehensive overview of mode-locked lasers using SWCNT-SA can be found in [21], showing the potential of SWCNT-SAs for mode-locking of solid-state lasers from 800 nm to 1940 nm. For OPSDLs, this would correspond to several different QW-materials: From GaAs QW for emission around 850 nm, over InGaAs QW in the range of 1 μm as used in this work, to GaInSb QW in the 2 μm region. SWCNT-SAs, on the other hand, can be manufactured on a variety of substrates in a cost-effective way by employing relatively simple techniques such as spray and spin-coating [22]. Moreover, they possess broadband ultrafast saturable absorption behavior, which either can be used in reflection or transmission. Note that the latter is not a trivial task to achieve with semiconductor saturable absorber structures [23].

However, it is not obvious that SWCNT-SAs can be employed for mode-locking OPSDLs due to low roundtrip gain and large non-saturable absorption loss as reported previously in a typical SWCNT-SA. In the present work, we demonstrate for the first time to our knowledge that saturable absorbers based on SWCNTs with low loss operating in transmission can be used for mode-locking an OPSDL. This first application of a SWCNT-SA for mode-locking of an OPSDL represents an important step for a further enhancement of the versatility of both devices and can be seen as an alternative, easy to implement and cost effective design. Stable fundamental mode-locking was obtained for such a system generating 1.23-ps pulses at a repetition rate of 613 MHz, delivering output powers of up to 136 mW near 1074 nm.

2. Experimental setup

In the present experiments, we employed a V-type cavity with a total length of about 244.5 mm (see Fig. 1). The cavity consisted of the gain structure in the first beam waist ($1/e^2$) of 60 μm and the SWCNT-SA for mode-locking placed in the second beam waist of 75 μm. A curved output coupler with a transmission of 0.6% and a radius of curvature (ROC) of 50 mm was used as the cavity end mirror. In addition, one highly reflective dielectric mirror with a ROC of 100 mm was utilized as the folding mirror to control the cavity mode waist. The semiconductor gain structure was grown by molecular beam epitaxy for the emission wavelength of 1060 nm. The structure includes a highly reflective Bragg mirror formed by 27 pairs of AlAs/GaAs layers and the gain region composed of 3 GaInAs quantum wells engineered for the emission wavelength of 1060 nm. The structure was grown in reverse order on an n-type GaAs substrate, which was etched away after the growth [24] and does not have a dielectric anti-reflection coating.

In the laser setup, the DBR of the semiconductor chip was capillary-force bonded on a 300-μm-thick CVD diamond heat spreader, which in turn was mounted on a water-cooled copper heat sink. During the experiment the heat-sink temperature was maintained at 15°C, in order to avoid condensation. The gain structure was optically pumped by a fiber-coupled 808 nm laser diode at an incident angle of 45°, focused to a spot size of 70 μm ($1/e^2$ radius).

#190130 - $15.00 USD Received 7 May 2013; revised 10 Jul 2013; accepted 10 Jul 2013; published 18 Jul 2013

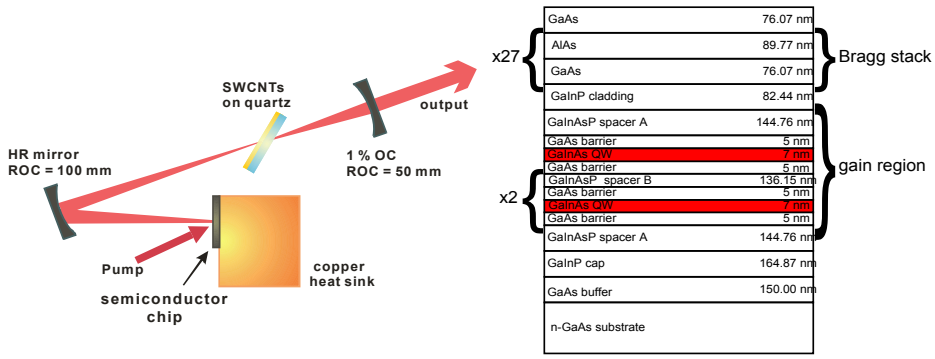

Fig. 1. Experimental setup of OPSDL and design of the gain structure.

For the OPSDL mode-locking experiment, a transmission-type SWCNT-SA was inserted at Brewster's angle into the beam waist of the cavity. The SWCNT-SA was fabricated in the following steps: The purified arc-discharge SWCNTs (Hanwha Chemical Co. Ltd., ~1.4 nm in diameter) were first dissolved in dichlorobenzene in a concentration of 0.1 mg/ml. The surfactant PmPV was added during an ultrasonic agitation to improve the solubility of the SWCNTs. After ultrasonication process, PMMA dissolved in dichlorobenzene was added to the SWCNT dispersion. The SWCNT/PMMA mixture was then stirred and centrifuged for about 12 hours. The well-dispersed mixture was finally deposited onto a 1-mm-thick quartz window by spin coating to form a homogeneous film. The thickness of the coated absorber layer was measured to be about 300 nm.

The fabricated SWCNT-SAs were characterized by linear and nonlinear transmission measurements. Single-pass transmission was measured using a spectrophotometer (Agilent Tech., Cary 5000) and a typical spectrum corrected for the Fresnel reflections is shown in Fig. 2. The broad absorption in the 1-μm and 1.8-μm regions is caused by the ensemble of the interband transitions in semiconducting SWCNTs of different diameters and chiralities [21]. The linear transmission at the laser operation wavelength of 1074 nm was about 99%. The nonlinear transmission measurement was performed by using a synchronously-pumped NIR optical parametric oscillator (OPO), delivering tunable sub-200 fs pulses at wavelengths between 1088 and 1590 nm. The modulation depth of the SWCNT-SA used was measured to be 0.25% and the saturation fluence (F_{sat}) 11.36 μJ/cm^2 at the shortest possible wavelength of OPO at 1088 nm (Fig. 3), whereas the linear and nonlinear characteristics of the SWCNT-SA in this region should not differ from those at the laser wavelength. The carrier recovery is also investigated by time-resolved pump-probe spectroscopy using the same OPO. The measured pump-probe trace was well-fitted with a biexponential function and delivered after deconvolution the fast and slow decay time constant of about 150 fs (limited by the excitation pulse duration) and 1.1 ps, respectively, corresponding to the intraband and interband transitions of SWCNTs (Fig. 3 (inset)) [25]. A more in depth description of SWCNT-SA fabrication and characterization can be found in [22].

#190130 - $15.00 USD Received 7 May 2013; revised 10 Jul 2013; accepted 10 Jul 2013; published 18 Jul 2013

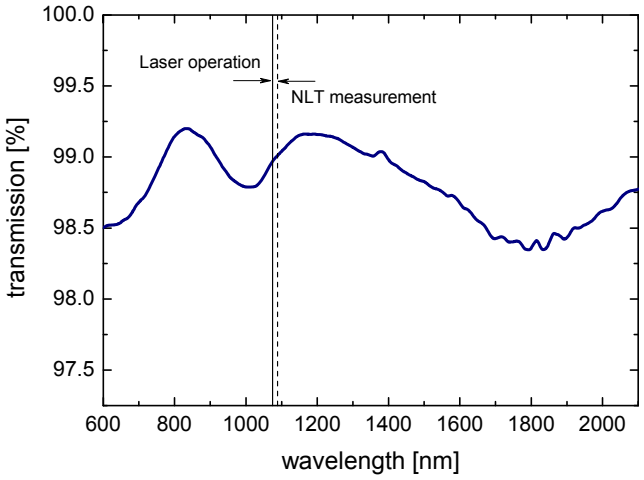

Fig. 2. Linear transmission of the SWCNT-SA with Fresnel-loss correction.

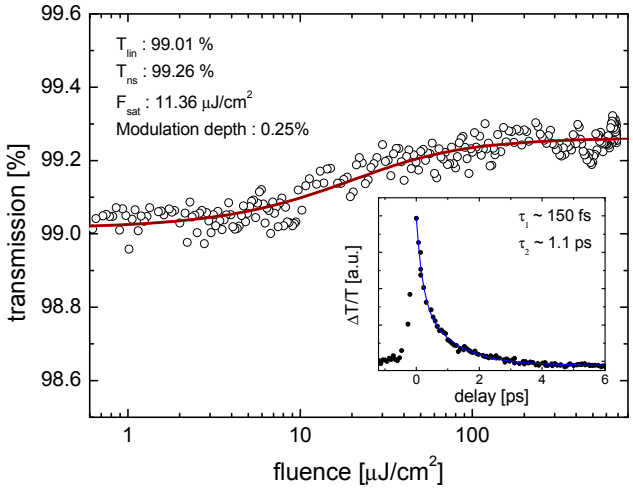

Fig. 3. Nonlinear transmission curve and (inset) pump-probe trace of the SWCNT-SA. The fit-function for the nonlinear transmission can be found in [26].

3. Results and discussion

We first investigated continuous wave (CW) operation of the OPSDL, before the SWCNT-SA was inserted into the cavity for mode-locking. A maximum average output power of 1.01 W at a pump power of 8.5 W was achieved, shown in Fig. 4(a). The slope efficiency in CW operation is limited by the undercoupling with a 0.6% transmission OC, which was specifically chosen to maximize the output power in the mode-locked regime. In addition, the slight decrease in the slope efficiency is related to the thermal rollover. The spectrum was measured with an optical spectrum analyzer with a resolution of 0.05 nm and found to be approximately 9 nm broad with a center wavelength of around 1074 nm (Fig. 4(b)). The modulation of the spectrum probably originates from an etalon effect of the gain chip.

#190130 - $15.00 USD Received 7 May 2013; revised 10 Jul 2013; accepted 10 Jul 2013; published 18 Jul 2013

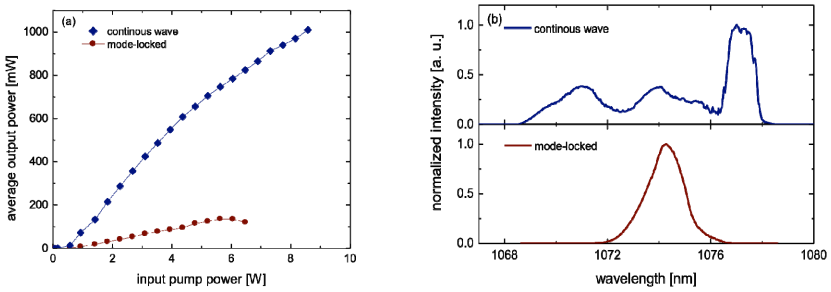

Fig. 4. (a) Average output powers and (b) laser spectra in cw and mode-locked operation at maximum output powers.

For mode-locked operation, the transmitting SWCNT-SA was placed at Brewster's angle between HR mirror and output coupler (OC) inside the cavity (Fig. 1). As shown in Fig. 3(a), the mode-locked maximum output power achieved was 136 mW with at a pump power of 6 W. The self-starting mode-locking could be achieved above the output power of 50 mW, where the calculated fluence on the absorber inside the cavity was 61 μJ/cm^2. This value is about five times higher than the saturation fluence (F_{sat} = 11.36 μJ/cm^2) of the SWCNT-SA used. At the maximum output power, the fluence was estimated to be 209 μJ/cm^2. At higher pump powers, the mode-locked operation was sustained, but the output power was slightly decreasing. Since no damage of the SWCNT-SA was observed, the mode-locked operation was probably limited by the thermal loading in the gain.

When the OPSDL is mode-locked, the spectrum becomes narrower down to a bandwidth of FWHM = 1.6 nm centered around 1074 nm. Compared to the modulated CW spectrum, the mode-locked case shows well-defined shape of spectrum without any modulation. The wavelength at maximum power is shifted by 13 nm from the nominal design wavelength because of an increase of the temperature in the gain structure under operating conditions. An intensity-autocorrelation measurement was performed to determine the pulse duration of the mode-locked pulses. The measured autocorrelation trace corresponded to a pulse duration of 1.23 ps (Fig. 5), with a small deviation of the fitted sech^2-pulse shape, which is usually used for passive mode-locking. The time-bandwidth product was about 1.6 times over the Fourier limit and no dispersion compensation was used inside the laser cavity. The total dispersion is given by the dispersion of the gain structure, which is around 50 fs^2 and by the dispersion of the quartz window with <100 fs^2. The laser was operating in TEM_{00} mode at all powers with a beam quality of M^2 = 1.2. The SWCNT-SA had to be aligned precisely at Brewster's angle. Due to the spin-coating process, the homogeneity of the sample was much better in the center of the sample, compared to the edges of the substrate.

#190130 - $15.00 USD Received 7 May 2013; revised 10 Jul 2013; accepted 10 Jul 2013; published 18 Jul 2013

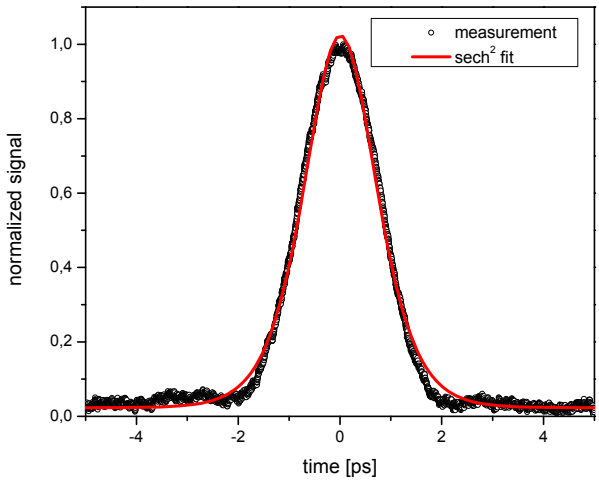

Fig. 5. Intensity-autocorrelation trace of the SWCNT-SA mode-locked OPSDL, resulting in a pulse length of 1.23 ps.

To verify the stable operation of the mode-locked OPSDL, radio frequency (RF) spectra were recorded with a biased InGaAs-photodiode with a bandwidth of 3 GHz. Top trace in Fig. 6 shows an average scan RF spectrum (over 100 scans) taken with the resolution of 3 MHz. The lower trace shows a single, high resolution scan with a resolution bandwidth of 3 kHz of the fundamental frequency, normalized to the carrier maximum. Both measurements confirm the stability of the pulse train and absence of multipulsing.

In order to unequivocally verify the mode-locked operation in this OPSDL, we performed external second harmonic generation (SHG) measurement. A 5-mm-long lithium triborate (LBO) crystal for type-I phase matching was used for frequency doubling of the mode-locked OPSDL. The linearly-polarized output was focused onto LBO using a broadband AR coated lens with a focal length of 25 mm, resulting in a focus of 50 μm ($1/e^2$ radius). At the maximum incident average power of 136 mW, an average SHG power of 10.56 mW was measured after a Schott BG 18 filter. The SNLO software (Sandia Nat. Labs) was used to estimate the expected SHG using plane-wave short-pulse mixing in LBO.

#190130 - $15.00 USD Received 7 May 2013; revised 10 Jul 2013; accepted 10 Jul 2013; published 18 Jul 2013

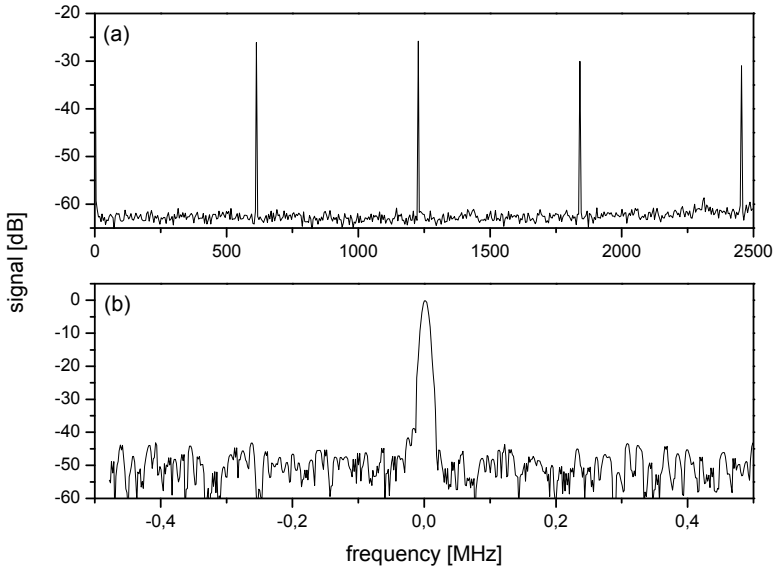

Fig. 6. RF spectra of the SWCNT-SA mode-locked OPSDL at 100 mW output power. (a) shows the frequency comb recorded with a resolution bandwidth of 3 MHz, averaged over 100 measurements. (b) shows a high-resolution single scan, recorded with a bandwidth of 3 kHz. The signal is normalized to the carrier maximum.

With an effective nonlinearity of 0.84 pm/V and the focus size of 50 μm ($1/e^2$ radius), the calculated theoretical efficiency is 10.8%. The experimental result was with 8.6%, taking into account the losses by the filter, close to the theoretical value. For comparison, we replaced the SWCNT-SA in the cavity by a plane quartz plate mounted at Brewster's angle to enforce single polarization in CW laser operation. Using 250-mW CW output from this laser in the same frequency doubling setup, a second harmonic power as low as 123 μW is generated as expected. This is a clear indication that the OPSDL operates mode-locked by the SWCNT-SA.

4. Conclusion

A passively mode-locked semiconductor disk laser was demonstrated where a transmitting SWCNT-SA mounted at Brewster's angle in the cavity was used as a mode-locker. This is to our knowledge the first result of mode-locking with carbon nanotubes in a semiconductor disk laser. The laser setup represents a highly practical and simple solution for a high repetition rate solid-state laser operating in the near-infrared spectral region near 1074 nm and delivered stable cw single pulse mode-locking with a maximum average output power of 136 mW at a repetition rate of 613 MHz. The corresponding pulse energy is 0.22 nJ. Without dispersion compensation, a pulse duration of 1.23 ps was achieved. A next step would be to lower the non-saturable losses in an optimized SWCNT-SA sample production process and show the versatility of this approach by using different QW materials like antimonite based gain structures in the 2 μm spectral region.

Acknowledgments

This work was supported by the Swedish Research Council (VR) through its Linnaeus Center of Excellence ADOPT and the European FAST-DOT project, and by the NRF funded by the Korean Government (MEST) (2011-0017494, 2010-220-C00013).

#190130 - $15.00 USD Received 7 May 2013; revised 10 Jul 2013; accepted 10 Jul 2013; published 18 Jul 2013